Accepted Manuscript

Flow characteristics of carbon fibre moulding compounds

A.D. Evans, C.C. Qian, T.A. Turner, L.T. Harper, N.A. Warrior

Flow characteristics of carbon fibre moulding compounds

A.D. Evans, C.C. Qian, T.A. Turner, L.T. Harper*, N.A. Warrior

Composites Group, Faculty of Engineering,

University of Nottingham, NG7 2RD, UK

*Email: lee.harper@nottingham.ac.uk

ABSTRACT

This paper presents the development of a low-cost carbon fibre moulding compound using an automated spray deposition process. Directed Fibre Compounding (DFC) is used to produce charge packs directly from low cost carbon fibre tows and liquid epoxy resin. A range of material and process related parameters have been studied to understand their influence on the level of macroscopic charge flow, in an attempt to produce a carbon fibre moulding compound with similar flow characteristics to conventional glass fibre SMCs.

Charge packs covering just 40% of the mould can be effectively used to process DFC, without detrimentally affecting void content, fibre distribution and mechanical properties. Tensile stiffness and strength values of 36GPa and 320MPa are reported for isotropic materials (100% charge coverage), which increase to 46GPa and 408MPa with flow induced alignment (50% charge coverage) at 50% fibre volume fraction.

KEYWORDS Compression moulding, SMC, Carbon fibre

1

1 INTRODUCTION

Compression moulding offers one of the fastest routes for the manufacturing of composite components from thermoset matrices. This makes sheet moulding compounds (SMC) the most widely adopted material format of fibre reinforced composites within the automotive industry, accounting for 70% of composites by mass [1]. The majority of these materials are derived from chopped glass rovings and mineral filled polyester resins, with limited composite stiffness (<15GPa) and strength (<100MPa) at low fibre volume fractions (<20%), making them unsuitable for structural applications such as automotive body and chassis components.

A number of manufacturers have exploited the mechanical properties of carbon fibres (CF), to produce advanced SMCs that are up to 300% stiffer than E-glass derivatives [2, 3]. The cycle time for these materials ranges from commonly 5-45 minutes, depending on part thickness and resin matrix type, and they have been used for a number of aerospace cabin, cargo, interior and secondary and tertiary structural component applications [4-7]. However, CF-SMC remains largely unexploited due to the high cost of raw materials and the cost of intermediate processing. It is typically based on chopped unidirectional (UD) prepreg, which offers fibre volume fractions approaching 60% [8], due to the efficient packing of the filaments within the UD chips. These materials are reported to be notch insensitive and exhibit a low sensitivity to defects [9, 10], as stress concentrations present at the bundle ends are often larger than geometrical stress concentrations resulting from the notch [11]. A high viscosity epoxy matrix is required to avoid fibre/matrix separation during moulding [12], which can be a particular problem for ribbed parts [13]. However, a high viscosity can limit macroscopic charge flow due to higher friction levels at the mould-composite interface [14], increasing the required moulding pressures. Initial coverage of the tool therefore tends to be

2

high (~80-90%), inevitably increasing the amount of touch-labour required to layup and position the charge, negating some of the advantages of using a moulding compound over a prepreg system.

Other CF-SMCs are produced using more traditional SMC manufacturing routes, by depositing and squeezing chopped fibres into a low viscosity resin paste [15]. Commercial products of this type tend to use polyester or vinyl-ester matrices to achieve good fibre wet-out, but require the addition of a thickening agent to increase the viscosity during compression moulding. The reaction of the thickening agent must be slow enough to ensure adequate wet-out of the fibre (and filler) during material manufacture. Local variations in concentration can cause large differences in thickening response, which can substantially influence moisture content [16, 17]. The flow characteristics of these industrial grade carbon moulding compounds have been optimised for lower tool coverage (charge initially covers 40-60% of the tool surface area), which is beneficial for incorporating features such as ribs and fasteners into complex geometries. Consequently the shape and position of the charge does not have to be precise, which reduces layup times and supports higher levels of automation for volume users. However, the interfacial shear strength between carbon fibre and vinyl-ester is typically poor compared with carbon/epoxy [18, 19], limiting the mechanical performance.

Epoxies can also be thickened, but not using the same type of agents commonly used for polyesters [20]. Many high performance epoxies can be formulated as B-staged systems, where the reaction between the resin and the curing agent is incomplete after mixing. Chemical or thermal B-staging partially cures the epoxy, but cross-linking is only fully completed when the system is reheated at a higher temperature. The viscosity is difficult to

3

control using B-staging, but it offers an opportunity to produce an affordable carbon fibre/epoxy moulding compound using low-cost raw materials.

The out-life (time at ambient temperature) of epoxy-based moulding compounds is also much lower than unsaturated polyester SMC, typically less than two weeks at room temperature [21]. This is a particular problem for high volume Tier one suppliers faced with refrigerating large quantities of material. Consequently, direct compounding processes have been developed to avoid the cost-intensive maturing stage and the problems associated with storage of traditional SMCs. Dieffenbacher's Direct SMC (D-SMC) process uses screw compounders to dispense a measured quantity of polyester resin, fillers and glass rovings [22, 23]. Similarly, Direct Long Fibre Thermoplastic (D-LFT) is an extruded chopped glass fibre thermoplastic moulding compound, suitable for high volume production of complex and large automotive body panels and semi structural components [24]. These methods are limited to fibre volume fractions of approximately 25%, in order to achieve good fibre wet-out inside the extruder screw, but offer tighter quality control and more flexibility in the compound formulation.

This paper investigates a new process for producing low cost carbon fibre/epoxy SMCs, which are capable of high levels of flow, enabling the manufacture of complex geometries. Directed Fibre Compounding (DFC) is used to produce carbon fibre/epoxy charge packs for isothermal compression moulding. DFC is an automated process that simultaneously deposits virgin carbon tows and a low cost liquid epoxy onto a tool surface. It is based on previous work by the authors and is a development of the Directed Carbon Fibre Preforming process (DCFP) [25-27]. DFC uses the same fibre chop and spray technology as DCFP, but a liquid resin is deposited simultaneously with the fibre to produce a material for compression

4

moulding, avoiding the separate resin injection phase typically associated with DCFP. The low resin viscosity ensures a high level of tow impregnation during spraying, minimising the risk of porosity developing during compression moulding. The charge is chemically B-staged to increase the viscosity of the matrix to ensure homogenous distribution of the fibre in the moulded component.

A range of material and process related parameters have been studied to understand their influence on the level of macroscopic charge flow, in an attempt to produce a carbon fibre moulding compound with similar flow characteristics to a glass/polyester system, i.e. initial charge coverage in the range of 40-60%. Lower charge coverage is desirable because it enables cycle times to be reduced, as fibre placement is less precise, relying on material flow to fill the mould tool. Controlling the initial charge shape also enables the local material properties to be tailored, as flow induced alignment can be introduced to enhance performance. Mechanical properties are presented for a range of charge sizes (initial percentage mould coverage) for a 1-dimensional flow scenario. These are compared against two commercial developmental CF-SMC benchmarks, a carbon fibre/epoxy SMC derived from chopped unidirectional prepreg and a carbon fibre/vinyl ester SMC.

2   DIRECTED FIBRE COMPOUNDING

DFC is an automated manufacturing process for producing 2D or 3D net-shaped moulding compounds. Chopped carbon fibre tows and liquid epoxy resin are sprayed simultaneously onto a low cost shell tool, which matches the geometry of one surface of the compression mould tool. The fibre/resin spray equipment is mounted on a 6-axis robot to deposit the material with minimal material wastage (<3% by mass) and high levels of repeatability.

5

Fibres are partially impregnated during the deposition stage of the DFC process, minimising the in-mould resin flow distance and therefore reducing the risk of large dry regions in the final component.

In a laboratory-scaled process, the carbon tow is fed into the chopper via a driven feed roller and then guided to the cutting roller, shown in *Figure 1*. A cone of randomly orientated chopped fibres is sprayed towards the tool surface. The fibre length can be changed during the deposition phase from 15mm to 75mm, by adjusting the speed ratio of the feed and chopper rollers. An atomised cone of liquid epoxy resin converges with the stream of fibres at the tool surface, wetting the fibre bundles to adhere them to the tool surface. The resin is pre-heated to achieve the optimum viscosity for spraying, which is then pumped to the delivery nozzle at the end of the robot arm.

DFC compounds are produced by spraying multiple layers of material to achieve the desired component mass, with local variations in thickness achievable according to the geometry of the tool. The maximum global volume fraction is 55%, as the level of macroscale voids dramatically increases for higher fibre content levels [28]. The deposition time is dependent on the robot path length, therefore tailored charges for more complex 3D geometries can be produced without significantly influencing the overall cycle time.

Once material deposition is complete, the charge is left to B-stage at ambient temperature before moulding. This is essential for minimising fibre-matrix separation during the compression stage and to enable the compound to be handled [16, 17]. The charge is removed from the carrier shell and inserted into a preheated matched mould tool. The shell tool is

6

cleaned and release agent is applied ready for the next charge. A flow chart of the DFC process is shown in *Figure 2*.

3 EXPERIMENTAL PROCEDURE

DFC charge manufacture

Toray T700-50C 12K carbon fibre was used for the current study, with 1% sizing content. This level of sizing was found to be suitable for achieving consistent fibre chopping. The tensile modulus of the fibre is 230GPa and the tensile strength is 4900MPa. The epoxy resin was a formulated system from Huntsman: Resin XU3508, Aradur 1571, Accelerator 1573 and Hardener XB3403 (100:20:3:12 by wt). The resin was preheated to 65°C to reduce the viscosity below 0.5Pas, ensuring good dispersion and wet-out of the chopped fibres.

Each DFC charge was sprayed onto a steel plate as a series of discrete layers, split into two orthogonal passes with a constant 50mm offset. The spray path was optimised to ensure uniform fibre distribution and to minimise any orientation bias from the chopping device [26, 27]. Freekote 700NC mould release agent was applied to the tool surface prior to spraying.

Chemical B-staging took place at ambient temperature for 24 hours, in accordance with the manufacturer's datasheets [29], which offered sufficient control over the level of staging. The viscosity was measured to be 50Pas after staging. It is possible however, to accelerate the staging by substituting the XB3403 hardener for a hot maturing agent. Staging times of ~5 minutes can then be achieved at 90°C.

7

An initial study was conducted to understand the influence of in-mould flow on the local fibre volume fraction, an assessment of fibre/matrix separation. *Table 1(a)* shows the DFC parameters used to produce moulding compounds with 40%, 60%, 80% and 100% mould coverages. Each charge was rectangular and placed along one edge of the tool to encourage a 1D flow regime. The initial position of each charge is indicated in *Figure 3.* The target fibre volume fraction, fibre length and linear robot travel speed remained constant at 45%, 25mm and 0.2m/s respectively. The carbon fibre tow feed rate, chopping rate, resin pump speeds and number of spray layers were adjusted to produce the required target areal mass of material for each mould coverage scenario.

The DFC machine parameters used for producing plaques to study the effects of fibre length and moulding pressure are shown in *Table 1(b)*. The target fibre volume fraction was constant throughout at 50%. A range of fibre lengths were investigated (15mm, 25mm, 50mm and 75mm) for different mould coverage levels (50%, 75% and 100%). The fibre feed rate, chopping rate, resin pump speed and number of spray layers were adjusted according to the required charge size (see values in *Table 1(b)*). The chopping rate was adjusted relative to the fibre feed rate in order to control the fibre length. The robot speed was constant (0.2m/s) for all fibre lengths greater than 25mm, but was reduced to 0.15m/s for the 15mm fibre length due to the gear ratio in the chopping device.

Benchmark materials

The novel DFC material is compared with two developmental CF SMCs produced by industrial partners; an epoxy-based system (EP-SMC) and a vinyl ester-based system (VE-SMC). The EP-SMC is derived from UD prepreg chopped into 50mm × 8mm chips, which are deposited randomly onto a release film mounted on a moving conveyor to form a sheet

compound with a fibre volume fraction of 54.8% ±2.5%. The compound uses AS4 carbon fibres with a tensile modulus of 230GPa and tensile strength of 4400MPa. The epoxy resin is a snap curing system which can be moulded in 3 minutes at 150°C and is suitable for automotive applications. A Tg of 125°C enables parts to be hot demoulded. The VE-SMC is produced by conventional glass compounding methods; using carbon fibre bundles with a tensile stiffness of 244GPa and a tensile strength of 4068MPa. Carbon fibres are chopped to 25mm and the matrix system has a continuous service temperature of 170°C, making it compatible with the E-coat process commonly used in the automotive industry. The fibre volume content of the VE-SMC is 40% ±2%.

Compression Moulding

Plaques were moulded in a 405×405mm square compression mould tool with a peripheral flash gap of 0.25mm. A tool closure speed of 1mm/s was used throughout to minimise fibre disruption around the edge of the plaques [30]. DFC plaques were moulded isothermally at 130°C for 30 minutes, followed by a 3.5 hour freestanding post cure in an oven. This moulding temperature was consistent for all DFC and commercial SMC moulds. The cure times for the EP-SMC and VE-SMC were 6 minutes and 30 minutes respectively, followed by a similar 3.5 hour free standing post cure. The mould pressure was 85 bar unless otherwise stated. Hard stops were used to avoid plaques tapering under non-uniform charge placement and to maintain constant plaque thickness. Plaques were produced from the VE-SMC and DFC materials using two charge coverage levels; 50% and 100%. EP-SMC was moulded at 80% coverage according to the manufacturer's recommendation.

Test procedures

9

Tensile testing was conducted according to ISO 527-4: 1997. *Figure 3* indicates the location of test coupons relative to the initial charge location. The cutting plan was designed to ensure that coupons were taken from both inside the original charge region and the flow region. Each tensile test specimen was 200mm $\times$ 25mm $\times$ 3.2mm with a gauge length of 100mm between the grips. Emery tape tabs were used to prevent slippage and minimise stress concentrations around the grip region. An extensometer with a 50mm gauge length was used to measure applied strains up to 0.4%. Subsequently, the cross-head displacement was used to calculate strains up to final failure. An extension rate of 2 mm/min was used.

Fibre volume fraction measurements were obtained by determining the composite density using ISO 1183-1: 2012. The density of the fibre and epoxy were $1.8g/cm^3$ and $1.2g/cm^3$ respectively, according to the manufacturer's data. The dry mass (in air) was measured for 25mm x 25mm samples, taken from the ends of each tensile test specimen, shown in *Figure 3*. The mass of the same samples was then recorded in water. The buoyancy force was calculated to determine the density of each specimen, taking into consideration the temperature of the water.

Void fractions were measured from micrographs taken from locations shown in *Figure 3*, at two different orientations (parallel and transverse to charge flow direction). Images were obtained at 5x magnification and processed using ImageJ software. A greyscale threshold was applied to each image to determine the void regions. The void fraction was measured in terms of area (%) for each image, and an average value was calculated from at 10 repeats for each scenario. Additionally, void size was reported in terms of the area of the largest void, measured in pixels and converted into millimetres.

4   ANALYTICAL MODELLING

An inclusion model has been used to predict the elastic constants and to determine the fibre orientation state for plaques manufactured for the charge coverage study. The closed-form expressions of the Mori Tanaka method [31] were reformulated by Qiu and Weng [32] to include the effects of anisotropic constituents, such as carbon fibre. Using the methodology outlined by the authors in [26], the Qiu and Weng model has been applied at 2 stages to firstly establish bundle properties, and secondly to predict unidirectional ply properties. Orientational averaging was applied at a third stage using the tensor approach of Advani and Tucker [33], to distribute the UD sub-units from Stage 2 according to a 3D spatial distribution.

The elastic properties of the bundles were calculated at Stage 1 using the elastic constants for carbon and epoxy taken from [32]. A tow volume fraction of 60% was assumed, similar to [26]. The fibre length was taken to be 25mm and the filament diameter was assumed to be 7μm. The transversely isotropic bundle properties from Stage 1 were then used to calculate UD ply properties at Stage 2, assuming the UD sub-unit had a volume fraction of 75% to account for the matrix material contained within the bundles from Stage 1. This yielded a global volume fraction of 45% to correspond with the experimental study.

The spatial orientation of a single bundle can be described by the Cartesian components (p_1, p_2, p_3) of a unit vector $\boldsymbol{p}$. A representative element of the present material contains many bundles of a constant length but different orientations, which can be described generally by the probability density function $\psi(\theta,\phi)$. ϕ describes the in-plane bundle orientations (in radians between $-\pi/2$ and $\pi/2$), which can be summarised by a double exponential distribution:

11

$$f(\phi) = \alpha \left(\frac{\exp\left[-\left(\dfrac{|\phi| - \mu}{\beta} \right) \right]}{2\beta} \right)$$

where μ is the location parameter, β is the shape parameter, α is the normalisation constant. This was previously used by the authors in [34] to describe the in-plane bundle orientations from a preforming process using similar spray deposition equipment. The in-plane fibre orientations are random in the 1-2 plane when β tends to infinity, and are aligned in the 1-direction when β tends to zero.

θ summarises the out-of-plane orientations in radians, using a trigonometric function in the form of

$$f(\theta) = a\sin^{2(b-1)}\theta$$

Equation 2

where a is a normalisation constant and b controls the shape of the out-of-plane distribution. This function was previously used in [26] to describe the out-of-plane orientations for a discontinuous carbon fibre material with 14mm long bundles. All of the fibres are aligned in the 1-2 plane when b is infinity. When b is unity the fibres are 3D random in space and when b is zero all of the fibres are aligned in the 3-direction (i.e. all fibres are out of the laminate plane).

The second and fourth order orientation tensors can be calculated by substituting the probability distributions from Equations 1 and 2 into Equations 3 and 4 respectively:

$$a_{ij} = \langle p_i p_j \rangle \equiv \int\limits_0^{2\pi}\int\limits_0^{\pi} p_i p_j \psi(\theta,\phi) \sin\theta \, d\theta \, d\phi$$

Equation 3

$$a_{ijkl} = \langle p_i p_j p_k p_l \rangle \equiv \int\limits_0^{2\pi}\int\limits_0^{\pi} p_i p_j p_k p_l \psi(\theta,\phi) \sin\theta \, d\theta \, d\phi$$

Equation 4

where $\langle \, \rangle$ denotes the orientational average.

Fibre orientation measurements are commonly performed using optical micrographs to determine both the in-plane and out-of-plane distributions. In-plane fibre orientations are derived from the length of the major and minor axis of the filament ends on a cast cross-section of the composite. Whilst image acquisition can be automated, specimen preparation is labour intensive, only small local sections are characterised and many samples are required to achieve a representative orientation distribution. This is a particular problem for the random bundled materials studied here because it is imperative that filaments are sampled from different tows. In-plane bundle orientations therefore need to be measured at the macroscopic component level and not the microscopic filament level. Kacir et al. [35] successfully used a highly visible dye on 250 glass fibres to identify orientations using digital images. This method is clearly inappropriate for opaque carbon fibres, so burn-off studies are typically performed on specimens to remove the resin [36], enabling the bundles to be removed consecutively. Whilst these macroscale methods can be successfully used to quantify bundle orientation effects, they are time consuming and accuracy can be limited.

Limited material availability prevented a destructive method from being used here to determine the orientation distributions. A sensitivity analysis has been performed to establish

13

the second and fourth order orientation tensors required to yield similar elastic constants from the Qiu and Weng inclusion model to those determined experimentally. Values of β and b have been adjusted until the longitudinal stiffness E_{11} was within 0.5% of the experimental value and the transverse stiffness E_{22} was within 5%.

5   RESULTS AND DISCUSSION

5.1   Comparison between DFC and other Carbon-SMC

A comparison of tensile properties is presented in *Figure 4* for all of the moulding compounds investigated. The red dotted line indicates the average of the longitudinal and transverse properties for the 100% coverage DFC plaque. The average tensile stiffness and strength was 36GPa ± 3.3GPa and 320MPa ± 27MPa respectively, at a moulded fibre volume fraction of 50%. This scenario has been used as a reference for comparison with other materials, as it avoids any uncertainty associated with flow induced alignment.

There is less than 3% variation between the longitudinal and transverse properties for the 100% DFC material, and error bars are small (<8%) confirming that the material is homogeneous and isotropic when moulded net shape (100% charge coverage), using the current specimen cutting plan (Figure 3). The longitudinal properties increase for smaller charge sizes (50% charge coverage), indicating flow induced alignment. The error bars remain low however, indicating good levels of fibre dispersion during flow. The properties of the DFC material are competitive against the commercial systems. The stiffness of the 100% DFC is comparable to the prepreg derived EP-SMC material, accepting there has been some fibre alignment in the commercial material due to the 80% initial charge. The stiffness of the 100% DFC is ~20% higher than the stiffness of the 100% VE-SMC as a result of the higher

14

fibre volume fraction (50% for DFC compared to 40% for VE-SMC). Furthermore, the strength of DFC is significantly higher than the other materials. For 100% charge coverage, the average ultimate strength for the VE-SMC material is 90MPa ± 25MPa, 72% lower than DFC. This can be partly attributed to the lower fibre strength (4068MPa) for the VE-SMC compared to the DFC (4900MPa), but also the poor interfacial bonding between the vinyl-ester matrix and the carbon fibre.

The fracture site for the 100% DFC coupons is relatively straight and perpendicular to the applied tensile load (see *Figure 5a*), indicating a fibre-dominated failure. This was observed for both longitudinal and transverse coupons, due to the high level of isotropy. Flow induced alignment in the 50% DFC coupons resulted in a combination of interface and fibre dominated failures, depending on the orientation of the specimen relative to the flow direction. Cracks at the interface propagated along the length of bundles at a lower stress than required to break the fibres, resulting in a matrix-dominated failure for specimens transverse to the flow direction (*Figure 5b*).

5.2 Effect of Charge Flow

There is a limit to the distance that compounds can flow during moulding before fibre/matrix separation occurs, as fibre agglomerations and entanglements prevent the matrix from carrying the fibres. The local fibre volume fraction variation has been measured across the width of each plaque in the flow direction. In general, *Figure 6* indicates that the fibre volume fraction varies by approximately ±5% across all plaques tested, including plaques with initial charge coverage as low as 40%. There is therefore no evidence of major fibre/matrix separation for the plaques tested.

In-mould flow of the DFC moulding compound causes the discontinuous fibre bundles to rotate and align in the flow direction. This causes a disparity in mechanical properties between the longitudinal (parallel to flow direction) and transverse (perpendicular to flow) directions. The level of flow is dependent on the initial size and shape of the DFC charge and therefore the mechanical properties can be tailored to some extent by encouraging charge flow, as shown in *Figure 7*. There is a clear linear trend between tensile stiffness and initial mould coverage, for both the longitudinal and transverse coupon directions. At 100% mould coverage, the material can generally be considered to be isotropic, with an average Young's modulus value of 34.3GPa for a fibre volume fraction of 45%. As the mould coverage is reduced to 40%, the longitudinal stiffness increases to 42.0GPa ± 3.3GPa and the transverse stiffness reduces to 21.8GPa ± 2.8GPa. There is no measurable increase in coefficient of variation in tensile modulus, indicating a homogeneous distribution of fibre across the plaque.

The tensile strength (*Figure 7b*) exhibits a similar general trend, increasing longitudinally and decreasing transversely as the mould coverage decreases. The calculated values have been determined from the strengths for the 100% mould coverage, assuming the same percentage differences for the smaller charge sizes as observed for the stiffness. The calculated values are within the experimental standard deviation values for all of the data points except the 40% coverage plaque. The strengths for the low coverage plaque (40%) are lower than expected, which can be attributed to an increase in out-of-plane fibre waviness with increased flow. Waviness is mostly observed in the boundary regions of the plaque, approximately one fibre length (25mm) from the edge, as shown in *Figure 8*. However, further analysis of the data showed no clear trend between the position of the test coupon (*Figure 3*) and the failure strengths recorded, as the ends of the specimens taken from the plaque edge were located in the jaws of the testing apparatus rather than the gauge section. The highest degree of waviness

16

can be observed in the 40% mould coverage specimens (*Figure 8a*), which tends to decrease as the level of in-mould flow decreases. The fibre bundles in the 100% mould coverage plaque are relatively planar (*Figure 8d*). These micrographs also confirm that the filaments remain in bundle form during flow and there are no matrix rich regions caused by fibre/matrix separation, so there are no signs of fibre agglomerations forming.

The influence of charge size, and hence increasing levels of flow, has been studied analytically, using the Qiu and Weng inclusion model [32] and an orientation averaging approach [33] to predict the in-plane elastic constants. *Figure 9* shows the influence of changing values for β and b on the longitudinal (E_{11}) and transverse (E_{22}) moduli. As β and b increase, the two in-plane moduli converge, as the fibre distribution tends towards being random in the 1-2 plane. The solid data points represent the experimental values and the percentages indicate the initial charge coverage values. Different values of b indicate changes in the out-of-plane orientation distribution. It is clear that each experimental data point corresponds with a different b value curve, indicating that the level of out-of-plane waviness changes in the experimental values, due to the reduction in charge size. This can be seen more clearly from *Table 2*, which summarises the tensor components required to yield equivalent tensile stiffnesses to the experimental values. Both the a_{33} and a_{3333} components increase as the charge size decreases, indicating greater levels of out-of-plane fibres. This observation corresponds with the micrographs shown in *Figure 8*, which confirm that the fibres become wavy as the flow distance increases.

The in-plane tensor components indicate that the level of fibre alignment increases in the 1-direction with reducing initial charge size. The second order component a_{11} for example, increases from 0.486 for the 100% coverage case to 0.610 for the 40% coverage case. The

17

tensor components for the 100% random case also indicate that there may have been some preferential alignment during the fibre deposition phase, as a_{11} and a_{22} are different (yielding different values for E_{11} and E_{22}). E_{22} is larger than E_{11} for the 100% coverage case, where the 1-direction was the expected flow direction. Greater gains in performance from flow induced alignment may be possible if the charge was to be rotated by 90° before moulding. The tensor components for this case were established using the E_{22} value, hence why the error between the experimental E_{11} value and the analytical prediction is higher than that for E_{22}.

5.3 Effect of Fibre Length

DFC plaques with fibre lengths ranging from 15mm to 75mm were manufactured at a fibre volume fraction of 50%, using 100% charge coverage. It is difficult to establish a trend between the tensile properties and increasing fibre length due to the high coefficient of variation. *Figure 10* indicates that 25mm is the optimum fibre length for 100% mould coverage, yielding the highest tensile stiffness and strength. However, all other data points are within one standard deviation, so the statistical significance of this trend is low. There is however, an increase in the coefficient of variation as the fibre length increases. This can be attributed to size effects [37], as a constant width test coupon was used for all fibre lengths according to ISO 527-4: 1997. Other studies in the literature have shown that increasing the specimen width relative to the fibre length would increase the tensile modulus but decrease the tensile strength [10, 11]; since the tensile modulus is a volume averaged property whereas the strength is dominated by critical flaws. The probability of a critical flaw increases as the volume of the coupon increases.

The effect of fibre length becomes more pronounced as the charge coverage decreases and the level of flow increases. *Figure 10* indicates that the ratio between longitudinal and transverse

properties generally increases as the fibre length decreases for smaller mould coverages. Shorter fibres are more susceptible to flow induced alignment than longer (75mm) fibres, particularly for smaller initial charges (50% compared with 100%). This has been previously discussed in terms of the Reynolds number [38], a measure of the inertial forces in the fluid, which is proportional to the fibre length. Long fibres cease to rotate when the Reynolds numbers is above a critical value and instead drift monotonically towards the shearing plane. However, compounds manufactured using 15mm long fibres did not flow as expected, as large dry patches formed. Chopping fibre bundles shorter increased the level of natural bundle fragmentation, as shown in *Figure 11*, effectively reducing the filament count per fibre bundle [26]. This consequently increased the loft (bulk factor) of the compound, increasing the compression forces required to close the mould tool [25] and reducing the permeability of the fibre architecture [39]. The number of fibre-fibre interactions also increases with shorter fibre lengths, increasing the frictional forces between the fibres, causing fibre bundle agglomeration and preventing fibre flow [40].

According to *Figure 10b*, the highest strength for the 50mm and 75mm fibre lengths is achieved when selecting a 75% charge size, compared to 50% charge for the shorter 25mm fibre length. This can also be attributed to fibre waviness. The longitudinal strengths of the 50mm and 75mm fibre length (50% coverage) plaques are superficially low, as the ultimate strength is limited by the degree of out-of-plane waviness, as previously shown in *Figure 8*. This is supported by the trend observed for the transverse strength, which consistently decreases with decreasing charge size.

5.4 Effect of Moulding Pressure

Plaques were initially manufactured using 100% charge coverage to isolate the effects of moulding pressure from fibre flow. ***Figure 12a*** shows that there was a reduction in both tensile stiffness and strength when the pressure was reduced from 85bar to 60bar. No further reduction in properties was observed however, when the pressure was reduced to 20bar. Reducing the moulding pressure influences the void content. ***Figure 12b*** confirms that the void content is higher (1.5%) for plaques moulded at 20bar, compared with those moulded at 85bar (1.0%). This directly influences the tensile strength, which decreases by 15% when the pressure is reduced from 85bar to 20bar. There are three requirements to achieve complete dissolution of trapped air: 1) high pressure, 2) high (local) flow rate and 3) low initial gas concentration [41]. During compression moulding of net-shaped compounds, the flow is negligible and the gas concentration is uncontrolled as a result of the atomisation stage of the liquid resin. Therefore, moulding pressure is the most influential factor controlling the level of voids, with higher pressures required to collapse any pockets of air.

A second study was conducted to understand the influence of moulding pressure for charge packs where flow was anticipated (i.e. less than 100% charge coverage). In addition, a range of fibre lengths was also investigated during this study to understand the combined effects of fibre length and mould pressure. Tensile properties presented in ***Figure 13*** show that both the stiffness and strength are generally higher for 50% coverage plaques moulded at 20 bar, compared with similar plaques moulded at 85bar. This is more pronounced for the longer fibre lengths, as the longitudinal strength increases by 33% for the 50mm fibres when the pressure is reduced from 85 bar to 20 bar and by 40% for the 75mm long fibres. Furthermore, the tensile moduli were also found to increase by 11% and 17% for the 50mm and 75mm fibre lengths respectively, when the pressure was reduced from 85 bar to 20 bar. Micrographs

(not shown) indicate an increase in fibre waviness for the longer fibre lengths, but there is also the possibility of increased fibre breakage due to increased fibre-fibre interactions, which increase at higher moulding pressures.

According to the results shown in *Figure 14*, charge flow improves the likelihood of air removal. The void content is lower for the 50% charge coverage plaques than the 100% net-shape plaques, for all fibre lengths tested. In addition, *Figure 14* also indicates that the void content is lower for plaques moulded at 20bar when the charge size is 50% (0.3%), compared with plaques moulded at 85bar with 100% coverage (1.0%). This also has the added benefit of reducing fibre waviness, as reported above.

6   CONCLUSION

A process to manufacture tailored charges suitable for high-volume compression moulding is investigated. Directed Fibre Compounding (DFC) overcomes the challenges of producing carbon fibre/epoxy moulding compounds using conventional compounding routes, to produce a structural material directly from low cost carbon fibre tows and liquid epoxy resin, eliminating the need for secondary manufacturing stages such as chopping UD prepreg. The process enables the charge to be specifically tailored for the intended application. Net-shape charge packs can be produced if no charge flow is required, which is of particular interest for future studies where DFC may be combined with prepreg compression moulding to produce a hybrid architecture. Conversely, the shape and position of the charge can be refined to encourage flow induced fibre alignment to enhance local material properties.

Tensile stiffness and strength values of 36GPa and 320MPa are reported for isotropic DFC materials, which increase to 46GPa and 408MPa with flow induced alignment (50% charge

coverage at 50% fibre volume fraction). These values compare particularly well against commercial carbon fibre compounds, including those derived from more expensive UD prepregs. A novel feature of the DFC material is that charge packs covering just 40% of the mould tool can be successfully used to produce plates with homogeneous fibre distribution. Analysis of local fibre volume fraction confirms that high levels of flow can be achieved without experiencing fibre/matrix separation. This has been enabled by using a B-staged epoxy, where the viscosity changes according to the degree of chemical conversion. Initially, a low viscosity during fibre/matrix deposition ensures high levels of bundle impregnation, whilst a higher viscosity after staging ensures fibre mobility during the compression moulding stage.

Furthermore, it has been shown that there are two dominant mechanisms for minimising porosity. Higher moulding pressures are required for net-shape (100% coverage) charges to collapse entrapped air, due to the lack of resin flow. Conversely, encouraging charge flow (smaller charge coverage) allows additional air to escape through the flash-gap, potentially enabling the moulding pressure to be reduced to achieve a high quality laminate. Lower moulding pressures also lead to reduced fibre waviness, particularly for longer fibre lengths, yielding higher tensile properties. There are clearly significant interactions between the variables studied here and it is therefore worth noting that increasing mould coverage, fibre length and moulding pressures concurrently does not necessarily produce the highest mechanical properties for these carbon moulding compounds.

7 ACKNOWLEDGEMENTS

8 REFERENCES

1. Alan Wheatley, D.W., Sujit Das, *Development of Low-Cost Carbon Fibre for Automotive Applications.* Advanced Composite Materials for Automotive Applications: Structural Integrity and Crashworthiness, 2014. **1**: p. 51-73.
2. Cabrera-Ríos, M. and J.M. Castro, *An economical way of using carbon fibers in sheet molding compound compression molding for automotive applications.* Polymer Composites, 2006. **27**(6): p. 718-722.
3. Bruderick, M., et al. *Applications of carbon/fiber SMC for the 2003 Dodge Viper.* in *Second SPE Automotive Composites Conference.* 2002.
4. Wulfsberg, J., et al., *Combination of Carbon Fibre Sheet Moulding Compound and Prepreg Compression Moulding in Aerospace Industry.* Procedia Engineering, 2014. **81**: p. 1601-1607.
5. Feraboli, P., et al., *Characterization of Prepreg-Based Discontinuous Carbon Fiber/Epoxy Systems.* Journal of Reinforced Plastics and Composites, 2009. **28**(10): p. 1191-1214.
6. Aubry, J., *HexMC — bridging the gap between prepreg and SMC.* Reinforced Plastics, 2001. **45**(6): p. 38-40.
7. *Boeing 787 features composite window frames.* Reinforced Plastics, 2007. **51**(3): p. 4.
8. McConnell, V.P., *New recipes for SMC innovation.* Reinforced Plastics, 2008. **52**(8): p. 34-39.
9. Feraboli, P., et al., *Defect and damage analysis of advanced discontinuous carbon/epoxy composite materials.* Composites Part A: Applied Science and Manufacturing, 2010. **41**(7): p. 888-901.
10. Feraboli, P., et al., *Notched behavior of prepreg-based discontinuous carbon fiber/epoxy systems.* Composites Part A: Applied Science and Manufacturing, 2009. **40**(3): p. 289-299.
11. Qian, C., et al., *Notched behaviour of discontinuous carbon fibre composites: Comparison with quasi-isotropic non-crimp fabric.* Composites Part A: Applied Science and Manufacturing, 2011. **42**(3): p. 293-302.
12. Dumont, P., et al., *Finite element implementation of a two-phase model for compression molding of composites.* Revue Européenne des Éléments, 2005. **14**(6-7): p. 885-902.
13. Dumont, P., et al., *Compression moulding of SMC: In situ experiments, modelling and simulation.* Composites Part A: Applied Science and Manufacturing, 2007. **38**(2): p. 353-368.
14. Guiraud, O., et al., *Rheometry of compression moulded fibre-reinforced polymer composites: Rheology, compressibility, and friction forces with mould surfaces.* Composites Part A: Applied Science and Manufacturing, 2012. **43**(11): p. 2107-2119.
15. Mason, K. *Compression molding with structural carbon SMC.* High-Performance Composites 2005 [cited 2015 7-5-15]; http://www.compositesworld.com/articles/compression-molding-with-structural-carbon-smc.
16. Gruskiewicz, M. and J. Collister, *Analysis of the thickening reaction of a sheet molding compound resin through the use of dynamic mechanical testing.* Polymer Composites, 1982. **3**(1): p. 6-11.
17. Saito, R., W.-M.J. Kan, and L. James Lee, *Thickening behaviour and shrinkage control of low profile unsaturated polyester resins.* Polymer, 1996. **37**(16): p. 3567-3576.
18. Kim, I.-C. and T.-H. Yoon, *Enhanced interfacial adhesion of carbon fibers to vinyl ester resin using poly(arylene ether phosphine oxide) coatings as adhesion promoters.* Journal of Adhesion Science and Technology, 2000. **14**(4): p. 545-559.
19. Vautard, F., L. Xu, and L. Drzal, *Carbon Fiber—Vinyl Ester Interfacial Adhesion Improvement by the Use of an Epoxy Coating*, in *Major Accomplishments in Composite Materials and Sandwich Structures*, I.M. Daniel, E.E. Gdoutos, and Y.D.S. Rajapakse, Editors. 2010, Springer Netherlands. p. 27-50.
20. Orgeas, L. and P.J.J. Dumont, *Sheet Moulding Compounds*, in *Wiley Encyclopedia of Composites*, L. Nicolais, A. Borzacchiello, and S.M. Lee, Editors. 2012, Wiley-Blackwell: New Jersey, United States. p. 2683-2718.
21. Kjelgaard, C., *Challenges in composites*, in *Aircraft Technology Engineering & Maintenance*. 2012, UBM Aviation Publications: London, UK. p. 52-57.

22. Rosato, D. *Automotive lightweighting process technologies to watch*. [cited 2015 21-8-2015]; http://multibriefs.com/briefs/exclusive/automotive_lightweighting_trend_3.html#.VdcsHflViko.

23. T. Potyra, D. Schmidt, and F. Henning, *New Direct Processing Technology for Thermoset Compression Moulded Composite Parts: Direct Strand Moulding Compound*, in *International Conference on Composite Materials 17*. 2009: Edinburgh, UK. p. 1-7.

24. Geiger, O., et al., *LFT-D: materials tailored for new applications.* Reinforced Plastics, 2006. **50**(1): p. 30-35.

25. Harper, L.T., et al., *Characterisation of random carbon fibre composites from a directed fibre preforming process: The effect of tow filamentisation.* Composites Part A: Applied Science and Manufacturing, 2007. **38**(3): p. 755-770.

26. Harper, L.T., et al., *Characterisation of random carbon fibre composites from a directed fibre preforming process: The effect of fibre length.* Composites Part A: Applied Science and Manufacturing, 2006. **37**(11): p. 1863-1878.

27. Harper, L.T., et al., *Characterisation of random carbon fibre composites from a directed fibre preforming process: Analysis of microstructural parameters.* Composites Part A: Applied Science and Manufacturing, 2006. **37**(11): p. 2136-2147.

28. LUCHOO, R., et al., *Net shape spray deposition for compression moulding of discontinuous fibre composites for high performance applications.* Plastics Rubber and Composites, 2010. **39**(3-5): p. 216-231.

29. *Resin XU 3508 / Aradur 1571 / Accelerator 1573 / Hardener XB 3403.* Huntsman Advanced Materials, July 2012.

30. Kotsikos, G. and A.G. Gibson, *Investigation of the squeeze flow behaviour of Sheet Moulding Compounds (SMC).* Composites Part A: Applied Science and Manufacturing, 1998. **29**(12): p. 1569-1577.

31. Mori, T. and K. Tanaka, *Average stress in matrix and elastic energy of materials with misfitting inclusions.* Acta Metallurgica, 1973. **21**: p. 571-574.

32. Qiu, Y.P. and G.J. Weng, *On the application of Mori-Tanaka's theory involving transversely isotropic spheroidal inclusions.* International Journal of Engineering Science, 1990. **28**(11): p. 1121-1137.

33. Advani, S.G. and C.L. Tucker III, *The use of tensors to describe and predict fiber orientation in short fiber composites.* Journal of Rheology, 1987. **31**(8): p. 751-784.

34. Harper, L.T., et al., *Fiber Alignment in Directed Carbon Fiber Preforms - Mechanical Property Prediction.* Journal of Composite Materials, 2010. **44**(8): p. 931-951.

35. Kacir, L., M. Narkis, and O. Ishai, *Oriented short glass fiber composites. I. Preparation and Statistical Analysis of Aligned Fibre Mats.* Polymer Engineering and Science, 1975. **15**(7): p. 525-531.

36. Trambauer, E.R., J.R. Hellman, and L.E. Jones, *Orientated microchannel membranes via oxidation of carbon-fiber-reinforced glass composites.* Carbon, 1992. **30**(6): p. 873-882.

37. WISNOM, M.R., *Size effects in the testing of fibre-composite materials.* Composites Science and Technology, 1999. **59**: p. 1937-1957.

38. Subramanian, G. and D.L. Koch, *Inertial effects on fibre motion in simple shear flow.* Journal of Fluid Mechanics, 2005. **535**: p. 383-414.

39. Endruweit, A., et al., *Random discontinuous carbon fiber preforms: Experimental permeability characterization and local modeling.* Polymer Composites, 2010. **31**(4): p. 569-580.

40. Kim, M.-S., et al., *Optimisation of location and dimension of SMC precharge in compression moulding process.* Computers & Structures, 2011. **89**(15–16): p. 1523-1534.

41. Lundström, T.S., *Measurement of void collapse during resin transfer moulding.* Composites Part A: Applied Science and Manufacturing, 1997. **28**(3): p. 201-214.

9 TABLES AND FIGURES

(a)

Target Vf (%)	45			
Mould coverage (%)	40	60	80	100
Fibre length (mm)	25			
Robot speed (m/s)	0.2			
Feed rate*	0.94	1.00	0.94	1.00
Chopping rate*	0.94	1.00	0.94	1.00
Resin pump speed*	0.94	1.00	0.94	1.00
No. of spray layers	8	5	4	3
Charge areal mass (gsm)	6480	4320	3240	2592
Initial charge area	162mm x 405mm	243mm x 405mm	324mm x 405mm	405mm x 405mm
Mould pressures (bar)	85			
Closing speed (mm/s)	1			

* Speeds normalised to 100% mould coverage (45% Vf, 25mm fibre length), highlighted red

(b)

Target Vf (%)	50											
Mould coverage (%)	50				75				100			
Fibre length (mm)	15	25	50	75	15	25	50	75	15	25	50	75
Robot speed (m/s)	0.15	0.2	0.2	0.2	0.15	0.2	0.2	0.2	0.15	0.2	0.2	0.2
Feed rate**	0.75	1.00	1.00	1.00	0.60	0.80	0.80	0.80	0.75	1.00	1.00	1.00
Chopping rate**	1.25	1.00	0.50	0.33	1.00	0.80	0.40	0.27	1.25	1.00	0.50	0.33
Resin pump speed**	0.75	1.00	1.00	1.00	0.60	0.80	0.80	0.80	0.75	1.00	1.00	1.00
No. of spray layers	6				5				3			
Charge areal mass (gsm)	5760				3840				2880			
Initial charge area	202.5mm x 405mm				304mm x 405mm				405mm x 405mm			
Mould pressures (bar)	20 and 85				85				20, 60 and 85			
Closing speed (mm/s)	1											

** Speeds normalised to 100% mould coverage (50% Vf, 25mm fibre length), highlighted red

Table 1: DFC and moulding parameters for (a) charge size study and (b) fibre length versus

moulding pressure study

	2D Random	100%	80%	60%	40%	2D UD
β	100000	3	1.65	1	0.75	1E-07
b	500	500	26	8	7	500
a_{1111}	0.375	0.362	0.404	0.430	0.476	1.000
a_{2222}	0.375	0.389	0.323	0.252	0.205	0.000
a_{3333}	0.000	0.000	0.001	0.009	0.012	0.000
a_{1122}	0.125	0.124	0.118	0.105	0.099	0.000
a_{1212}	0.125	0.124	0.118	0.105	0.099	0.000
a_{1133}	0.000	0.000	0.010	0.030	0.036	0.000
a_{2233}	0.000	0.000	0.008	0.020	0.019	0.000
a_{1313}	0.000	0.000	0.010	0.030	0.036	0.000
a_{2323}	0.000	0.000	0.008	0.020	0.019	0.000
a_{11}	0.500	0.486	0.532	0.565	0.610	1.000
a_{22}	0.500	0.514	0.449	0.376	0.323	0.000
a_{33}	0.000	0.000	0.019	0.059	0.067	0.000
E_{11} (GPa)	34.92	33.94	36.99	38.50	42.14	92.70
E_{22} (GPa)	34.92	36.06	30.70	24.71	21.22	6.47
G_{12} (GPa)	13.10	13.02	12.47	11.36	10.83	2.32
v_{12}	0.33	0.32	0.28	0.22	0.18	0.02
Experimental E_{11} (GPa)		32.45	36.91	38.32	42.00	
Experimental E_{22} (GPa)		36.16	29.62	24.44	21.79	
Error E_{11}		4.40%	0.23%	0.48%	0.34%	
Error E_{22}		-0.28%	3.52%	1.09%	-2.67%	

Table 2: Summary of tensor components for DFC plaques with decreasing initial charge coverage (shown as percentage values). Corresponding stiffnesses are presented from the Qiu and Weng model and compared against the experimental values. Tensors for 2D random and 2D UD are included for reference.

26
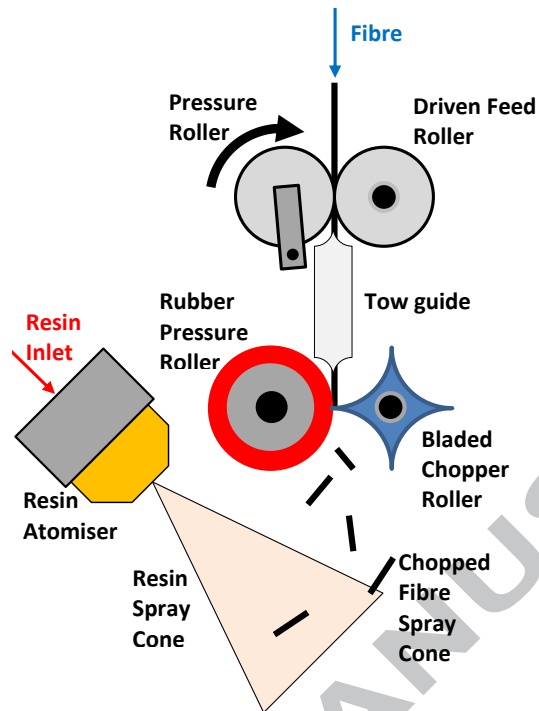
Figure 1: DFC end effector fitted to robot arm,
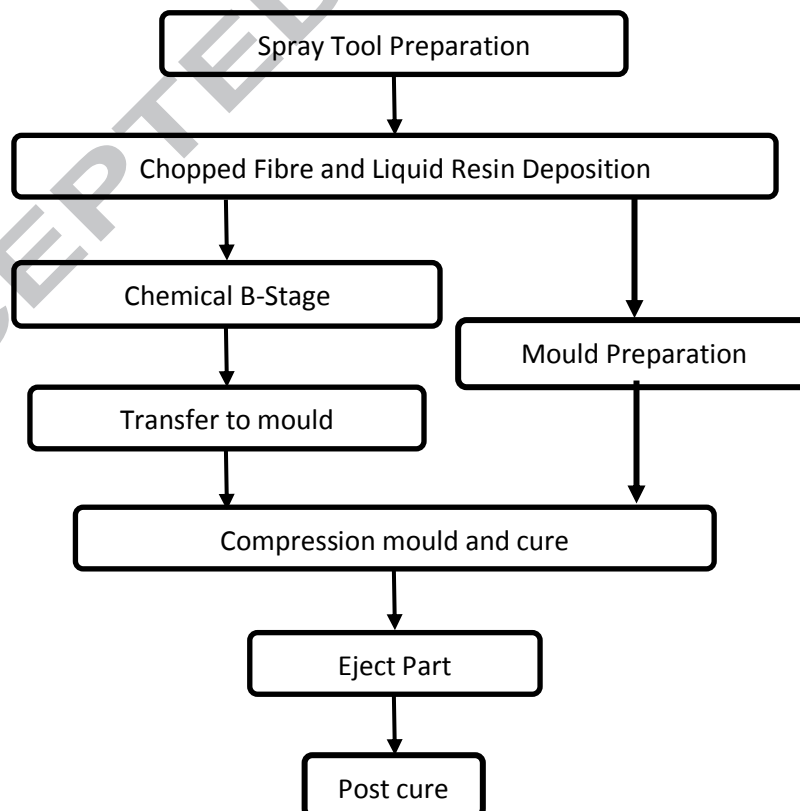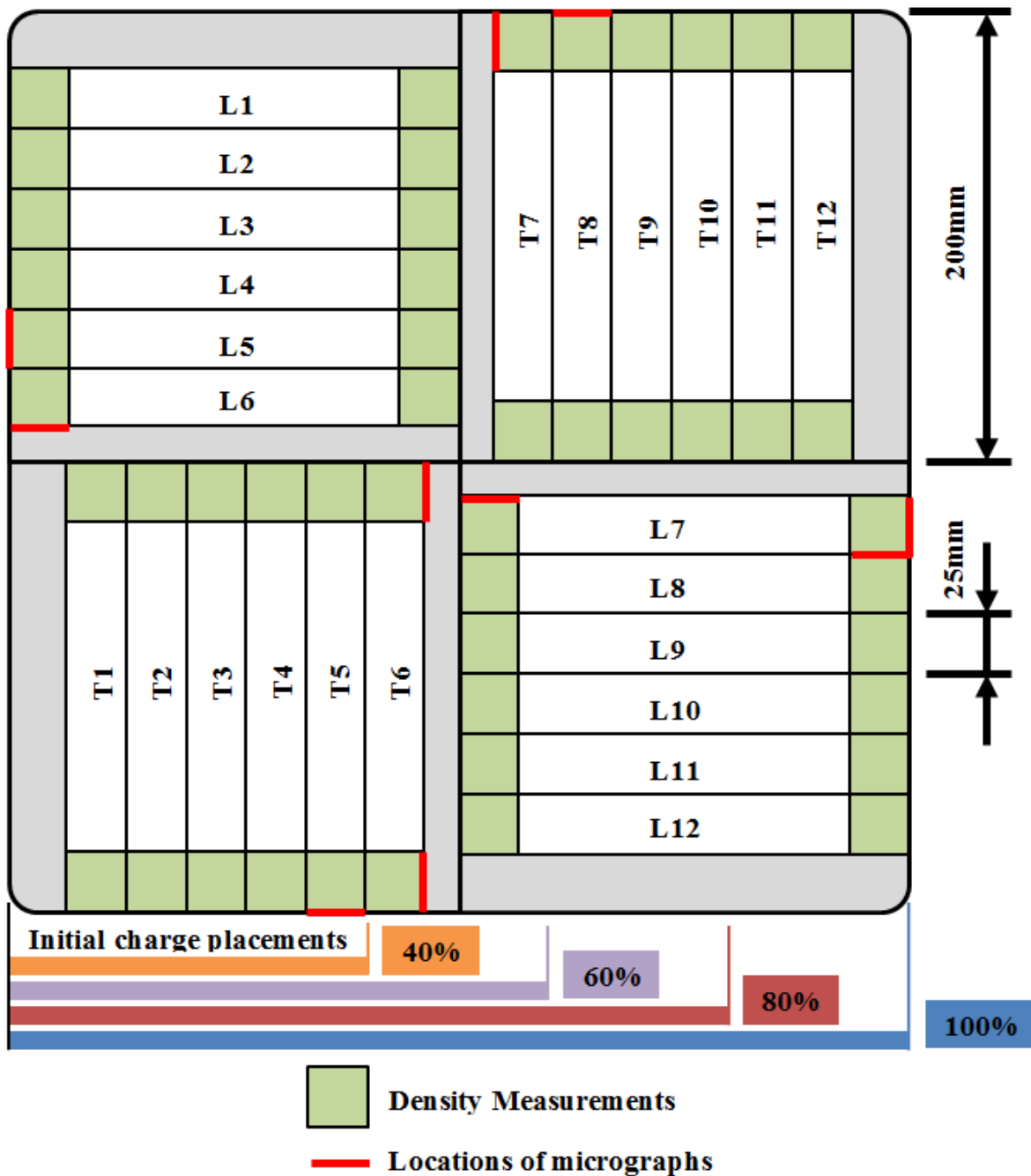

Figure 2: DFC flow chart

27

Figure 3: Initial charge position and cutting plan for the 405mm x 405mm plaques. Locations for tensile coupons, density measurements and micrograph shown.
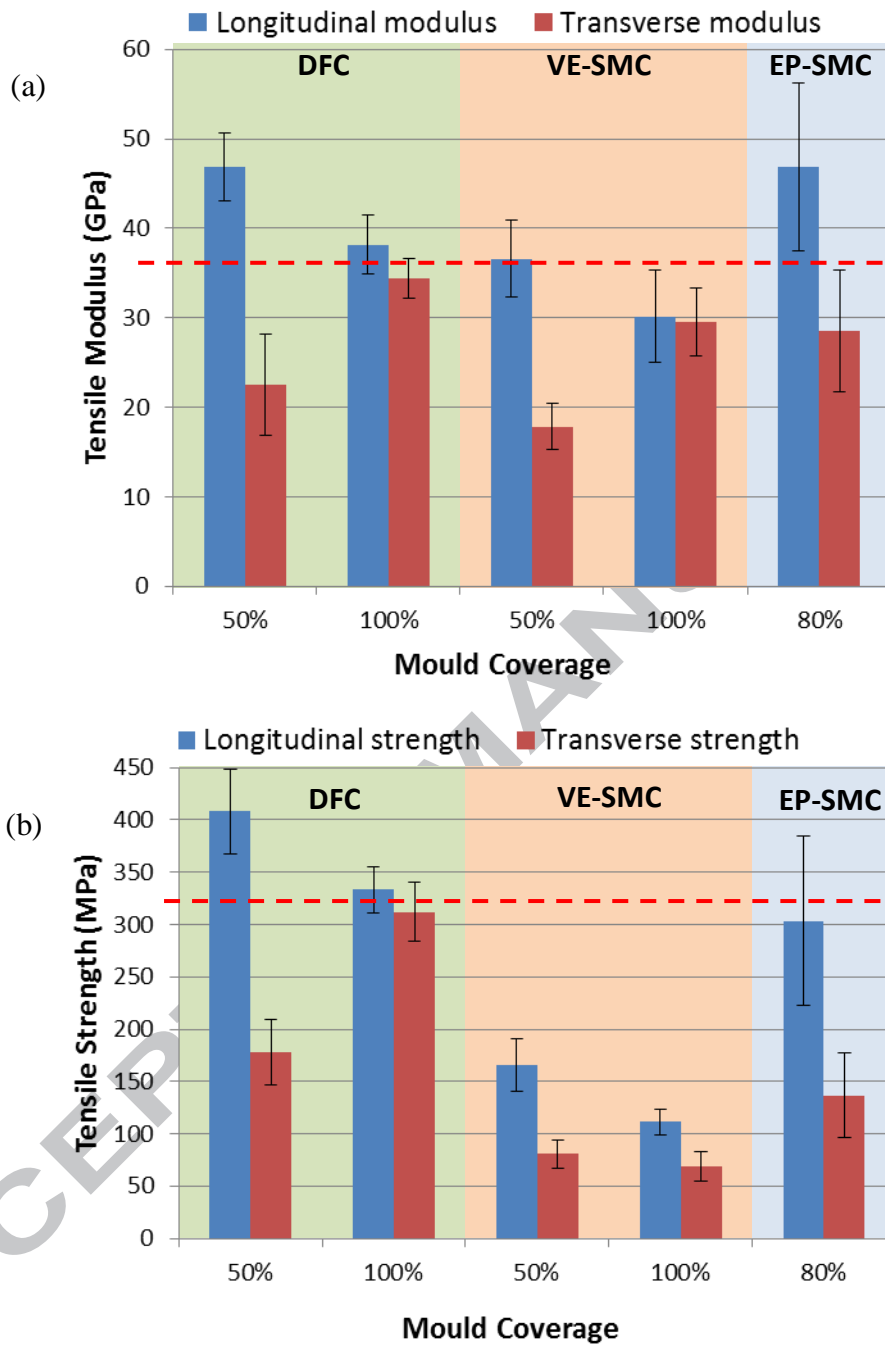
Figure 4: Tensile modulus (a) and tensile strength (b) as a function of mould coverage. All materials moulded at 85 bar. The red dotted line represents the average of the longitudinal and transverse properties of the 100% coverage DFC material.

a)

b)

Figure 5: Typical failure mechanisms experienced during tensile failure of longitudinal

specimens of (a) 100% mould coverage DFC, (b) 50% mould coverage DFC
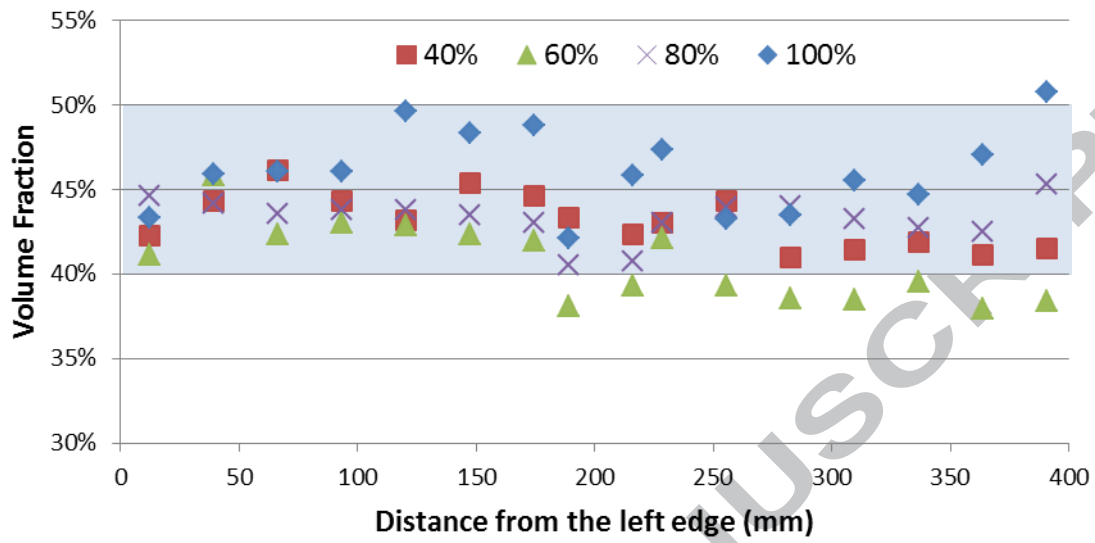
Figure 6: Fibre volume fraction measurements at positions from the left plaque edge (x = 0mm), to the right edge (x = 400mm) for different percentage mould coverages. Initial charge placement was on the left and flowed in one dimension to the right.

31
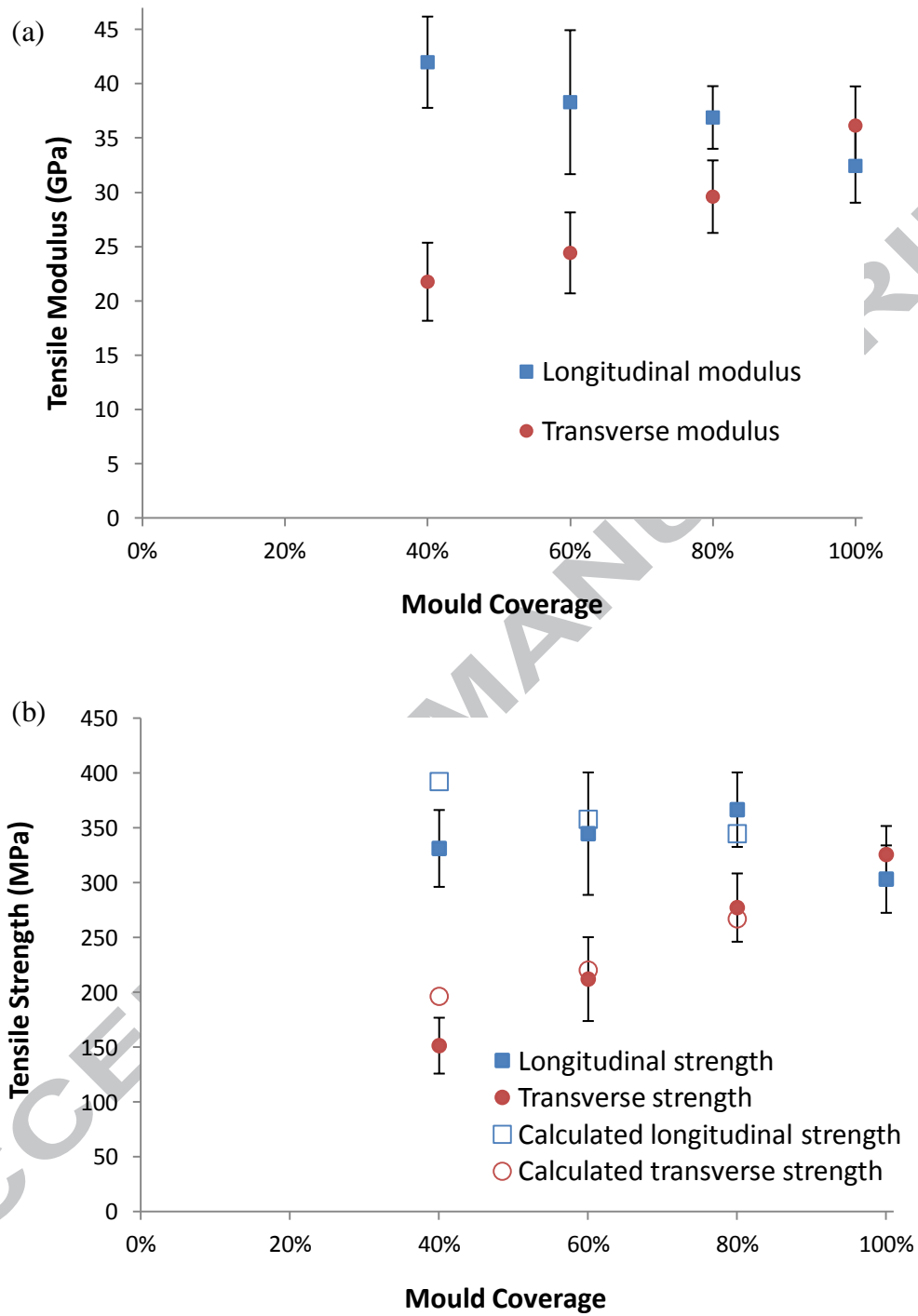
Figure 7: Tensile modulus (a) and strength (b) of DFC plaques. (25mm fibre length, 45% Vf)
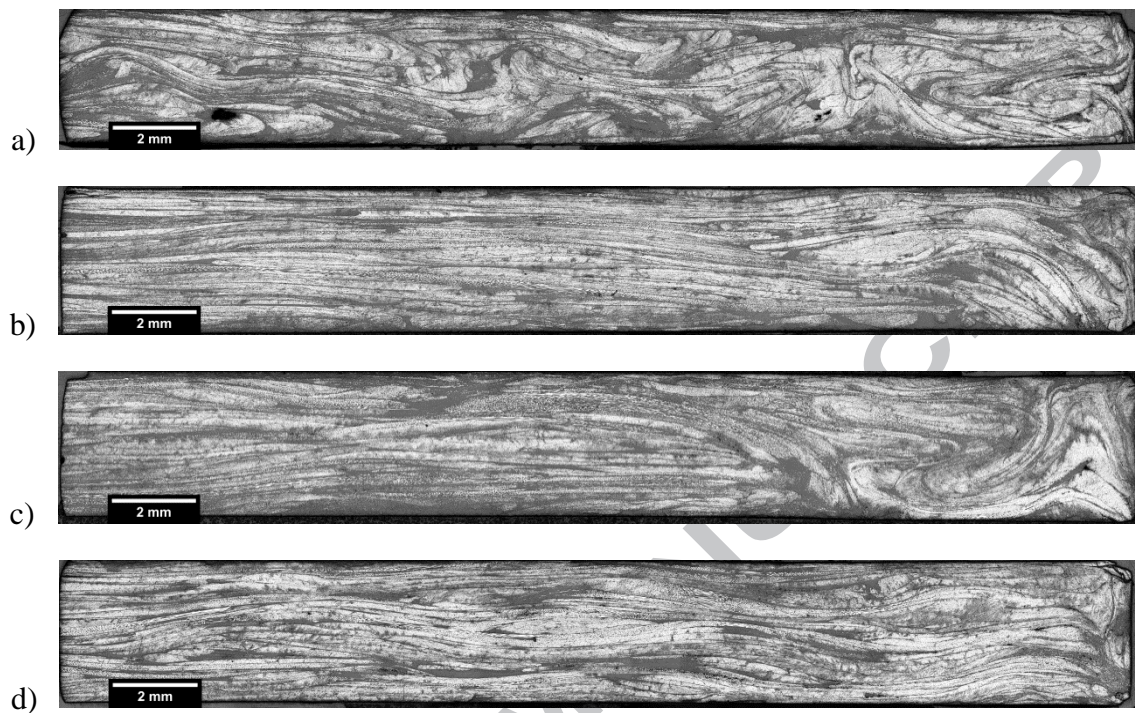
Figure 8: Micrographs (5x magnification) of the right hand edge, end of flow, for 40%

(a), 60% (b), 80% (c) and 100% (d) mould coverages. All images are parallel to the flow

direction
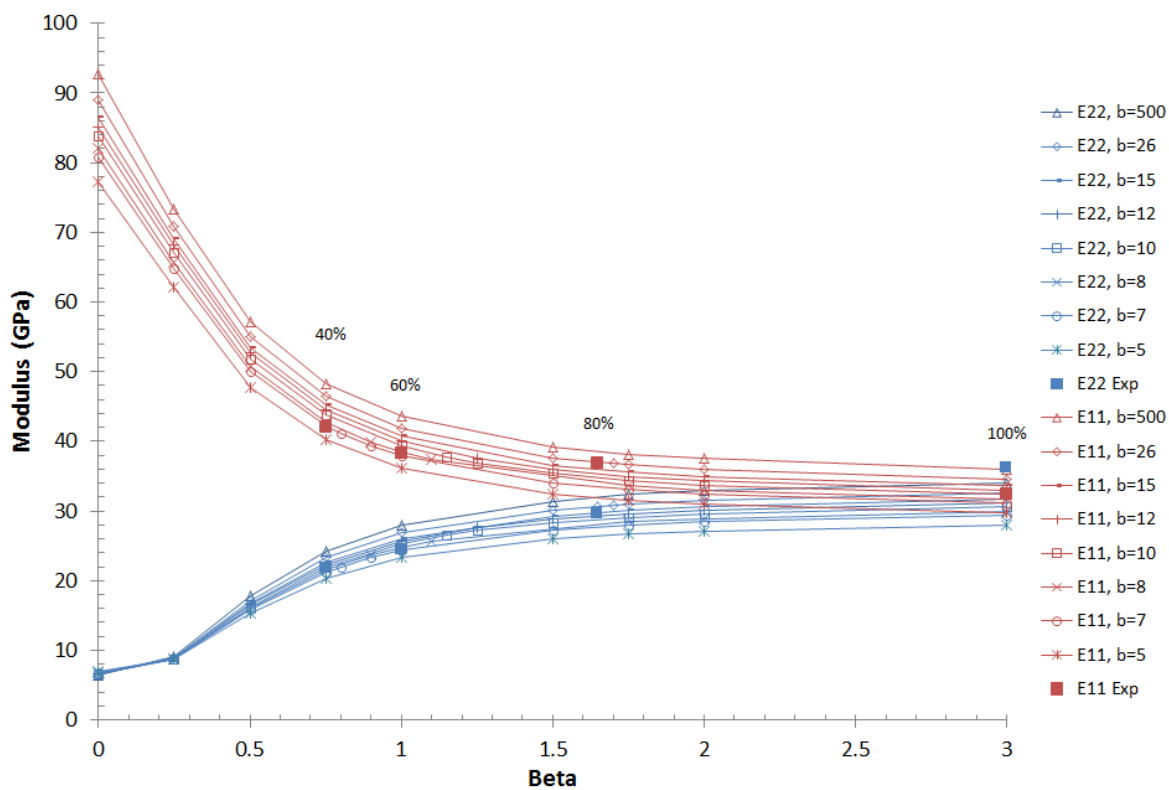
Figure 9: Effect of β on the tensile modulus for a range of b values. Percentage values indicate the level of charge coverage
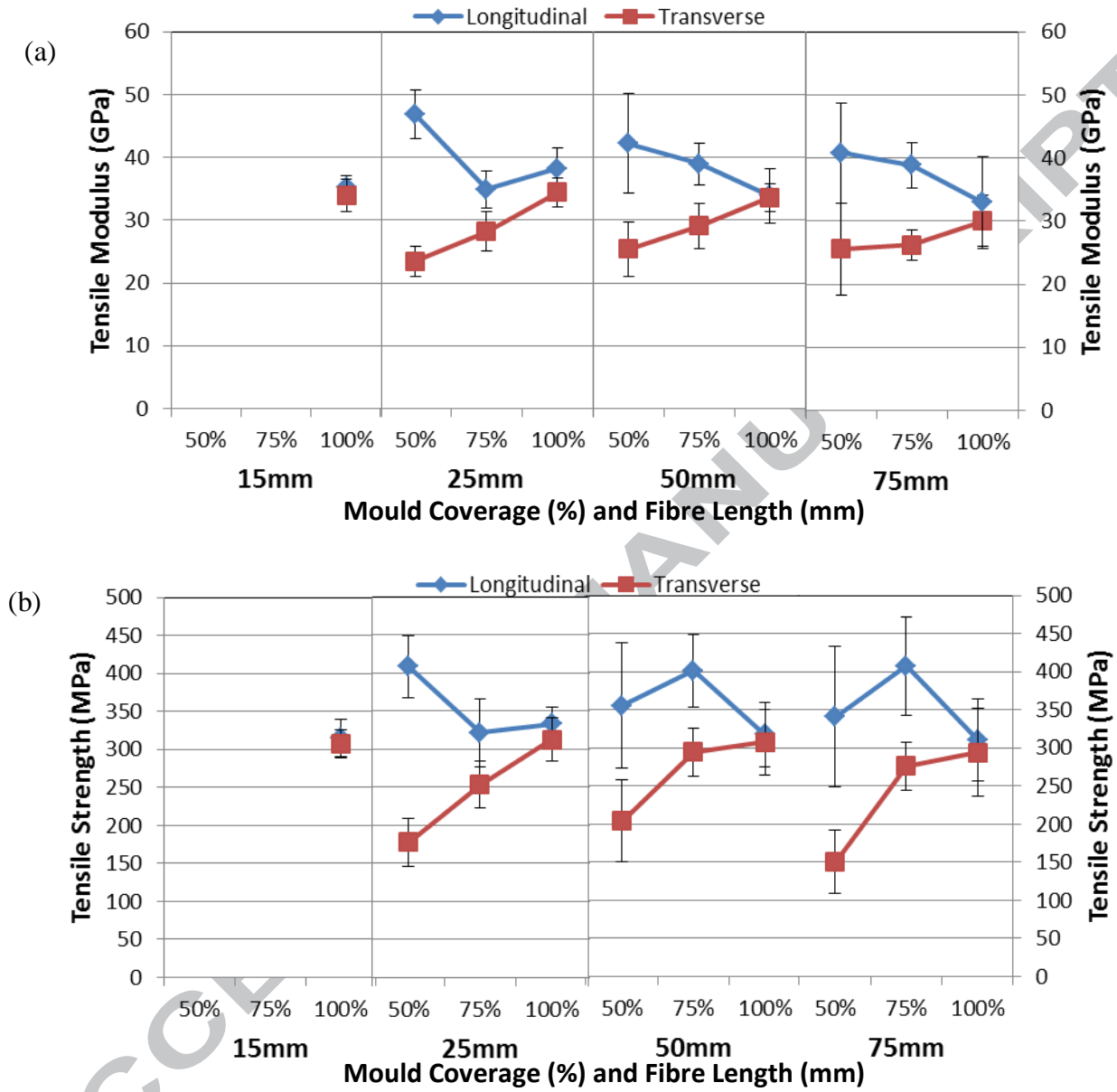
Figure 10: Effect of fibre length on tensile modulus (a) and tensile strength (b) for DFC compounds with 50%, 75% and 100% mould coverages (50% Vf).

35
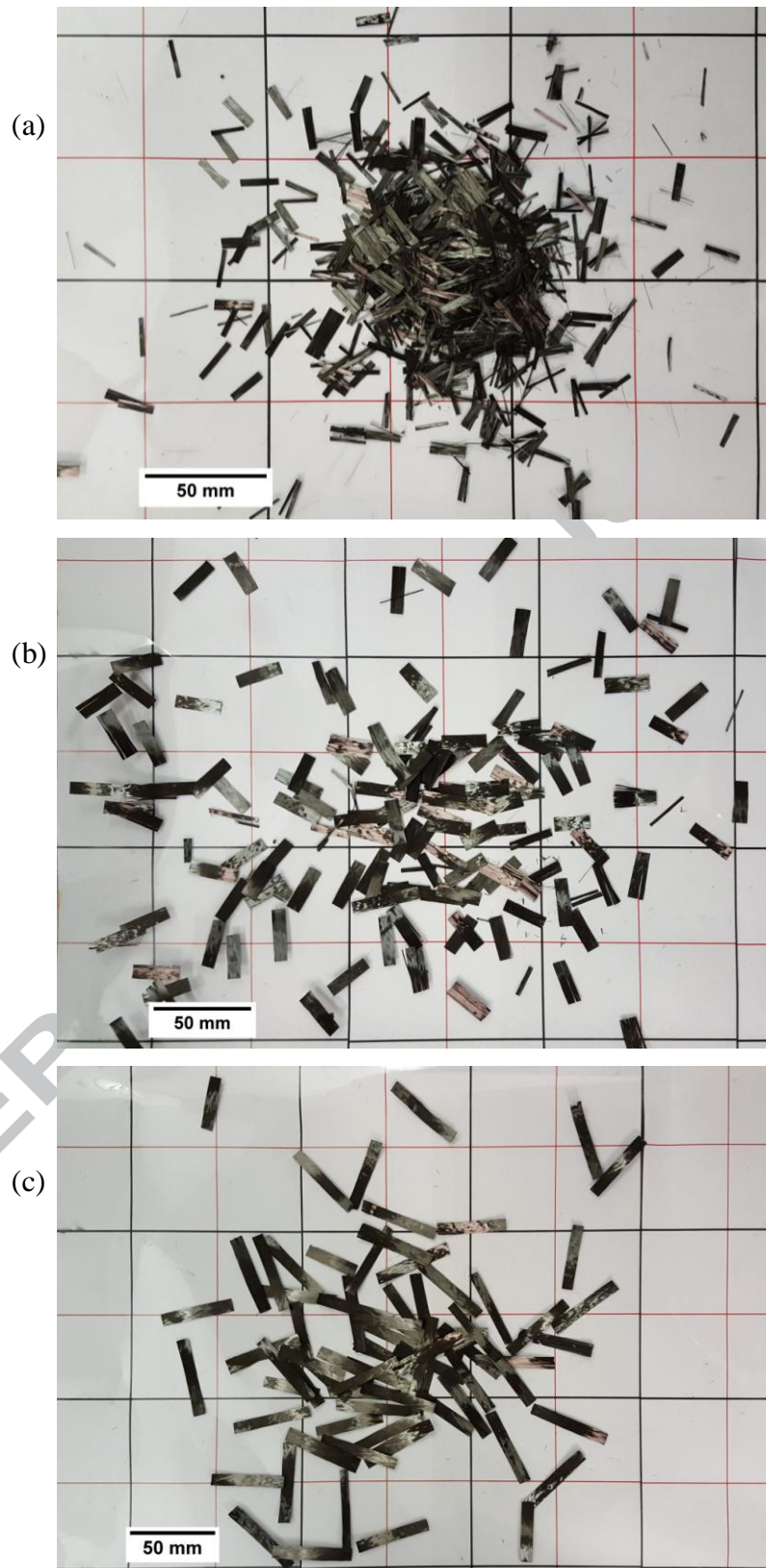
Figure 11: Dry deposition of (a) 15mm (b) 25mm and (c) 50mm fibre lengths, showing

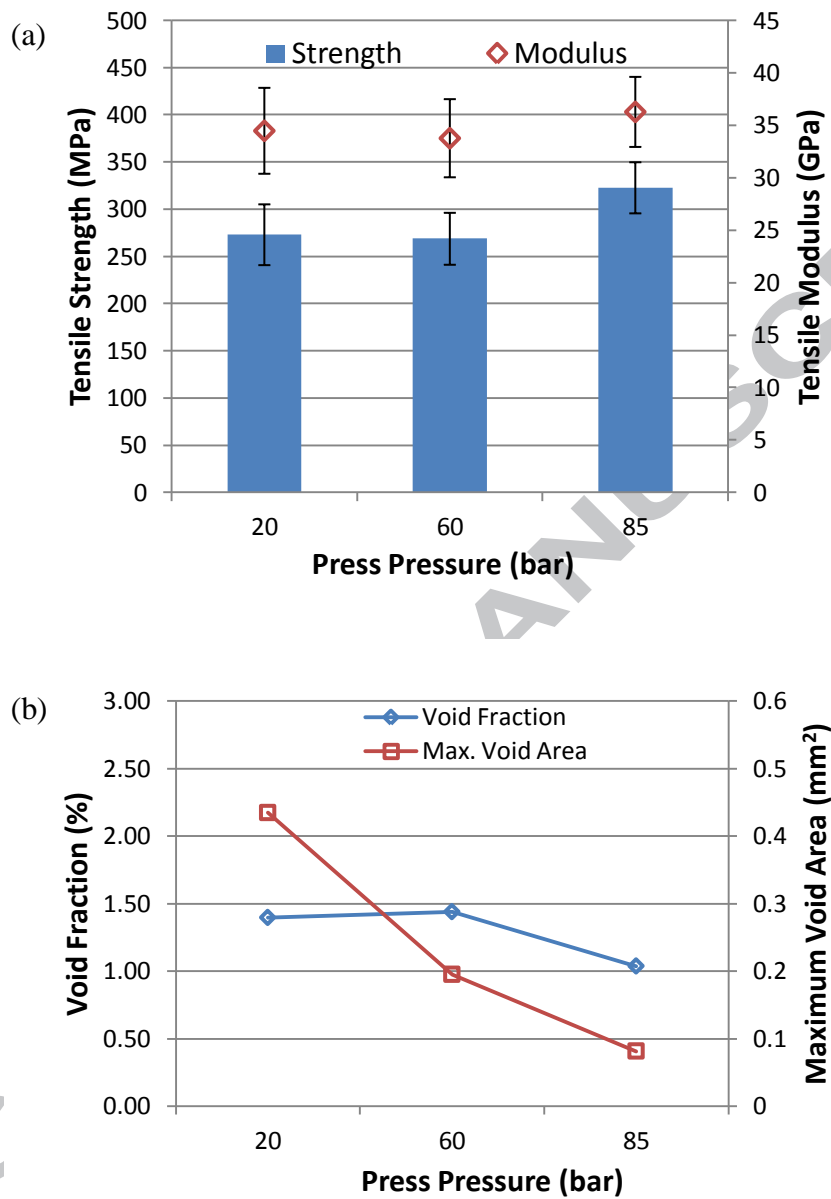increasing levels of tow fragmentation for shorter bundle lengths.

Figure 12: The effect of mould pressure on tensile properties (a) and void content (b) for
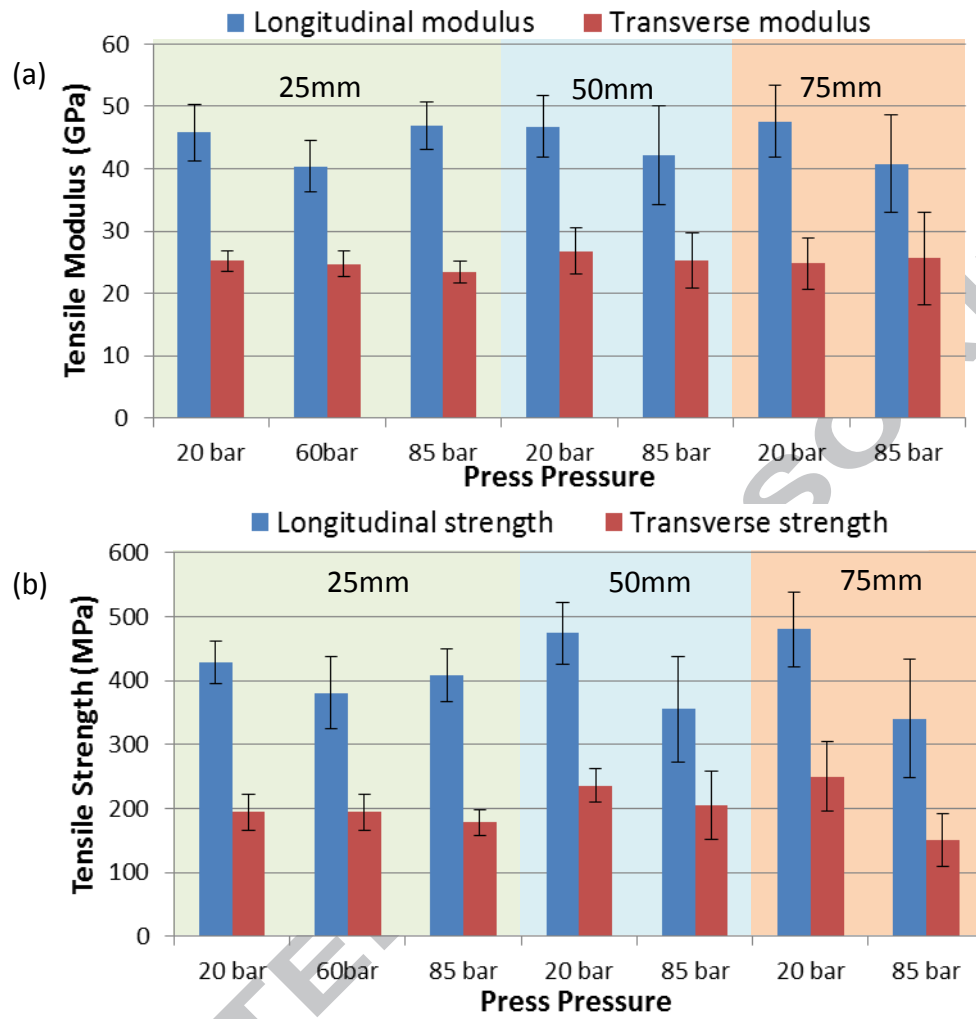
100% net-shaped compounds

Figure 13: Tensile modulus (a) and strength (b) of different fibre length DFC compounds

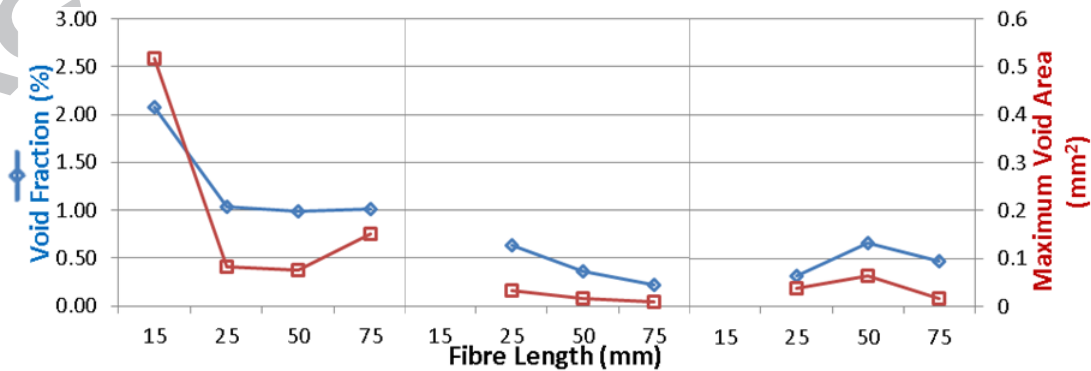with 50% mould coverage and 50% Vf, varying the moulding pressure.

Figure 14: Void content for varying fibre lengths for 100% charge coverage at 85 bar (left),

50% charge coverage at 85 bar (middle), and 50% charge coverage at 20 bar (right)

38